# A Self-Biased Low Modulation Index ASK Demodulator for Implantable Devices

Xiao Sha\*, Yuanfei Huang\*, Tutu Wan\*, Yasha Karimi\*, Samir Das<sup>†</sup>, Petar Djurić\* and Milutin Stanaćević\*

\*Department of Electrical and Computer Engineering, Stony Brook University, Stony Brook, NY 11794

†Department of Computer Science, Stony Brook University, Stony Brook, NY 11794

Email: xiao.sha@stonybrook.edu

Abstract—Free floating sub-mm and mm sized brain implants can communicate through a backscatter-based link in a presence of the EM field generated by the external coil. This link reduces the bandwidth requirement in the uplink communication of these implants to the external coil and enables a close-loop operation of the distributed implant system through reduced latency. The critical challenge in the link design stems from the low modulation index in the incident signal at the receiving coil. This calls for the design of the ASK demodulator that can resolve signals with low modulation index. We propose a demodulator design comprising a self-biased common-source based envelope detector that provides sufficient conversion gain and at the same time operates with a low power consumption. With 90 MHz carrier frequency and 50-kbps data rate, the ASK demodulator, implemented in 65 nm CMOS technology, resolves input RF signal with 1% modulation index consuming less than 100 nW when amplitude of the input RF signal is 200 mV.

Index Terms—Implantable medical devices (IMDs), amplitude shift keying (ASK) demodulator, ultra-low power consumption, low modulation index, self-biased.

## I. INTRODUCTION

The research efforts in the design of brain implantable devices and their use in a wide range of neurological diseases have been steadily growing [1], [2]. We envision a departure from the conventional approach of recording neural signals that employs wireless microelectrode arrays (MEA) in favor of a distributed array with a large number of distinct microimplants that cover a relatively large area of the brain [3]-[6]. This sub-mm or mm sized, free floating wireless implants minimize the impact of the implant on the surrounding tissue [7], [8]. In the design of these implants, providing wireless power to the device and data communication link are critical parts of the distributed system design. In a conventional approach, the implantable device that senses the neural data uploads the recorded data to an external device. When the power consumption is the critical parameter and the data rate is lower than 100-kbps, the uplink communication channel is conventionally implemented by backscattering [1], while for uplink with higher data rate a range of communication techniques have been used [9]-[12]. When the number of the implanted devices grows, as in the case of free floating submm sized implants, the communication link between implants and a single external device is time-multiplexed. This greatly reduces the communication bandwidth of a single implant to the external device.

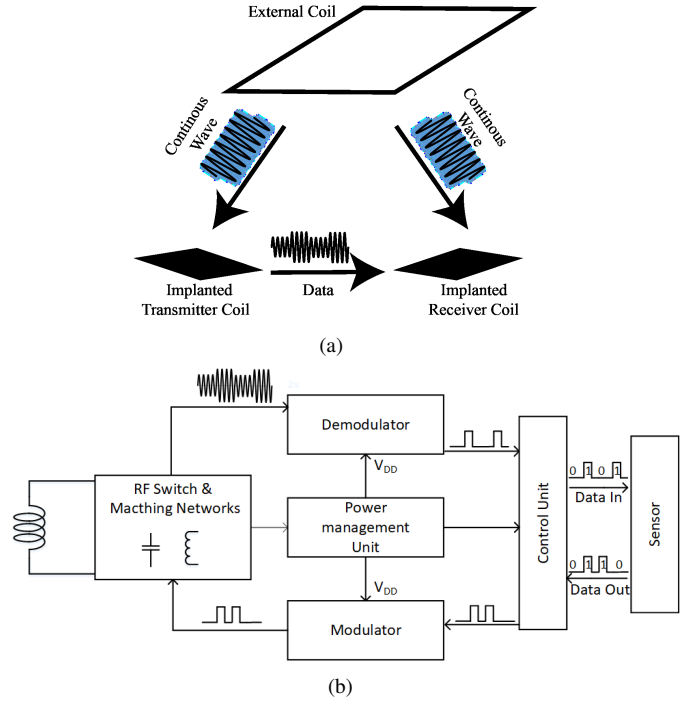


Fig. 1. (a))Illustration of the implant coil to implant coil inductive communication link in the presence of the external coil. (b) Block diagram of the implantable device.

A backscattering technique that in the presence of a RF signal in the environment enables communication between RF tags at ultra-low power consumption has been demonstrated in applications like smart spaces [13]. To reduce the bandwidth of the communication channel with the external device and enable a closed-loop system, the implants can be designed to communicate with the neighboring implants via backscatter [14] in a scenario illustrated in Figure 1(a). The block diagram of such implant is shown in Figure 1(b). An impedance matching network precedes the demodulator and power management unit in order to have the same resonant frequency as the external coil. The demodulator converts input modulated waveform to the baseband signal and is followed by the control unit that recovers the digital data from the input waveform.

In the backscatter-based implant to implant link, the input signal at the receiving implant is a combination of the signal directly received from the external coil and a modulated signal reflected from the transmitting coil. The reflected signal is significantly lower than the directly received signal and this results in a combined signal with the low modulation index [14]. Common source(CS) based ASK demodulators have been commonly proposed due to conversion gain they provide [15], [16], however the power consumption in these structures has been higher than the required limit. We propose a self-biased structure that preserves the gain at the lower power cost.

The rest of the paper is organized as follows. Section II describes the architecture of the ASK demodulator. The overall design methodology for the proposed the circuit is elaborated in the same section. Section III presents the simulation result, followed by the conclusions in Section IV.

#### II. DEMODULATOR IMPLEMENTATION

The feasibility of the backscatter-based implanted coil to implanted coil inductive link in the presence of the external coil has been analyzed and demonstrated [14]. For the mmsized coils with the link data rate of 10s kbps, the highest power transfer efficiency and link distance are achieved at operating frequency of 90 MHz. The modulation index in the received signal in the backscatter-based links depends on the received power at both transmitting and receiving coils and the mutual inductance between the coils. In order to achieve a link at the maximum distance between coils and for different orientation of the coils, a demodulator that can resolve low modulation index in the received signal is required. The proposed design of the ASK demodulator comprises a commonsource(CS) envelope detector, shown in the Figure 2(a), and a two-stage dynamic comparator, shown in Figure 2(b). The envelope of the differential input RF signal,  $V_a$ , is extracted at the output of the CS stage,  $V_{env}$ , and the low-pass filter that follows generates  $V_{avq}$ .  $V_{avq}$  provides a reference voltage for the comparison with the envelope signal required for the demodulation of the input signal, as well as the biasing voltage for the CS stage.

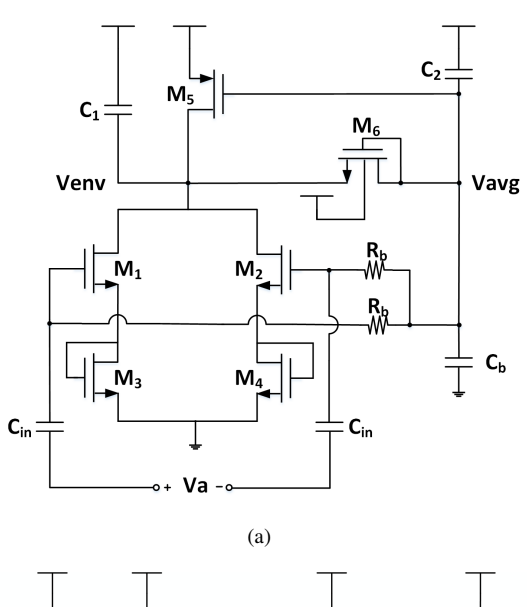
## A. CS-based Envelope Detector

The input differential RF signal,  $V_a$  is ac-coupled to the pseudo-differential common-source stage with the input transistors  $M_1$  and  $M_2$  and source degeneration introduced by the diode-connected transistors  $M_3$  and  $M_4$ . The transistors  $M_3$  and  $M_4$  provide a feedback to minimize variation in the biasing current and enable self-biasing of the envelope detector. The transistors operate in the subthreshold region of the operation across the full range of the amplitude of the input RF signal, providing the maximum nonlinearity. The current of the transistor operating in subthreshold region, assuming that the drain to source voltage is higher than 100 mV, is

$$I_d = I_{so} \frac{W}{L} \exp(\frac{V_{gs} - V_{th}}{mU_T}) \tag{1}$$

where  $I_{so}$  is

$$I_{so} = \mu C_{ox}(m-1)U_T^{2}$$
 (2)



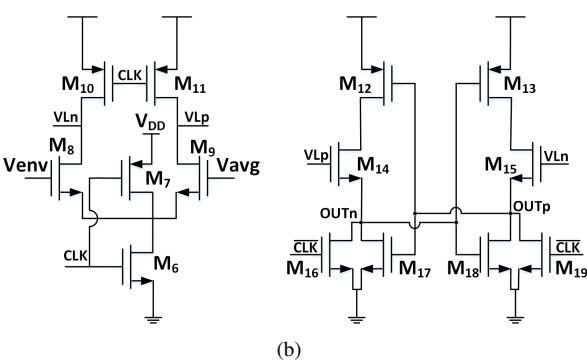


Fig. 2. (a)Proposed self-biased ASK demodulator. (b)Energy efficient two-stage comparator.

 $\mu$  is mobility,  $C_{ox}$  is oxide capacitance, m is subthreshold slope factor,  $U_T$  is the thermal voltage (= KT/q, 26mV at room temperature), W is transistor width, L is transistor length,  $V_{gs}$  is gate to source voltage and  $V_{th}$  is transistor threshold voltage.

The conventional CS-based envelope detector with an externally supplied biasing voltage for the input transistors [16] requires generation of multiple biasing voltages. The bias voltage is selected based on the amplitude of the RF signal. An adaptive biasing circuit that resolves a wide range input signal with a small modulation index can be used [15]. However, keeping constant biasing current introduces a significant cost in terms of the extra power consumption at low input amplitude, illustrated in Figure 3. The proposed solution is self-biased with a slightly lower conversion gain. The output voltage  $V_{avq}$ , obtained after the low-pass filter, formed by MOS-bipolar-pseudo resistor  $M_6$  and  $C_2$ , is used as the biasing voltage. When the sinusoidal RF input signal  $V_a \cos(\omega t)$ is superimposed on the input bias  $V_{avg}$ , with the increase in the input amplitude  $V_a$ ,  $V_{avg}$  will decrease and provide higher supply current in  $M_5$ , avoiding the output voltage be forced by the high gain to the negative saturation. And  $V_{avq}$ increases to save power consumption at small input amplitude as show in Figure 3, and biases the entire circuit at suitable

 $\label{table I} TABLE~I$  Design parameters of the proposed ASK demodulator

M <sub>1.2</sub>	M <sub>3.4</sub>	$M_5$	M <sub>6</sub>	$C_{in}$	$C_h$	$C_1$	$C_2$	$R_b$
$[\mu m/\mu m]$				[pF]			$[k\tilde{\Omega}]$	
0.7/1.8	0.5/1.8	3.8/1	10/1.5	0.5	9.5	0.13	15	190

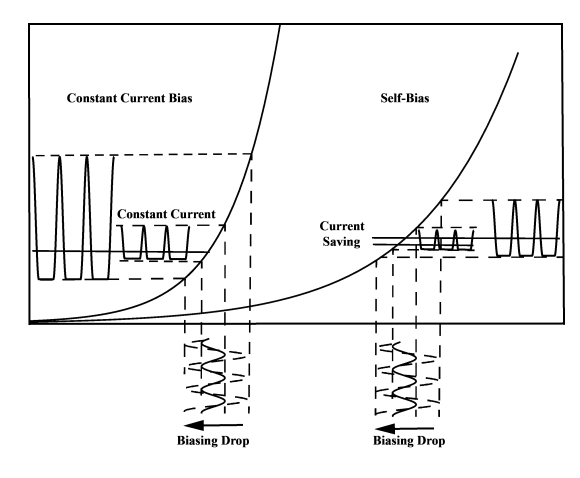


Fig. 3. Example illustrating of operation principal between previous [15] and our structure.

operation point. The pseudo-differential implementation of common source architecture cancels odd terms in the output current and results in a rectified output current that can be approximated as [16]

$$I_{out} \approx \frac{V_a^2}{8(mU_T)^2}. (3)$$

By properly sizing the transistors, a high enough constant conversion gain can be obtained in a wide input amplitude range. The sizing of the transistors and the values of the passive components is listed in Table I.

# B. Comparator Design

The implementation of 2-stage comparator comprising a dynamic pre-amplifier followed by a dynamic latch, with  $V_{env}$  and  $V_{avg}$  as inputs, is shown in Figure 2(b) [17]. The advantage of differential operation is that the voltage difference between  $V_{env}$  and  $V_{avg}$  only needs to be accurate during the sample phase. The edge alignment issue between clock and signal is solved by controllable delay cells [18]. Additional reset PMOS is added, resulting in less net kickback charge into envelope detector [19]. The 100 kHz clock can be generate by on chip 100 nW uncompensated oscillator [20], and is shared by the entire chip.

#### III. SIMULATION RESULTS

The proposed ASK demodulator was designed and simulated in 65 nm CMOS technology. Simulations are performed with 50-kb/s ASK modulated RF input signal with amplitudes ranging from 0.1~V to 1.2~V with modulation indexes (MIs) of 1% and 5%. The 90 MHz carrier frequency is adopted [14].

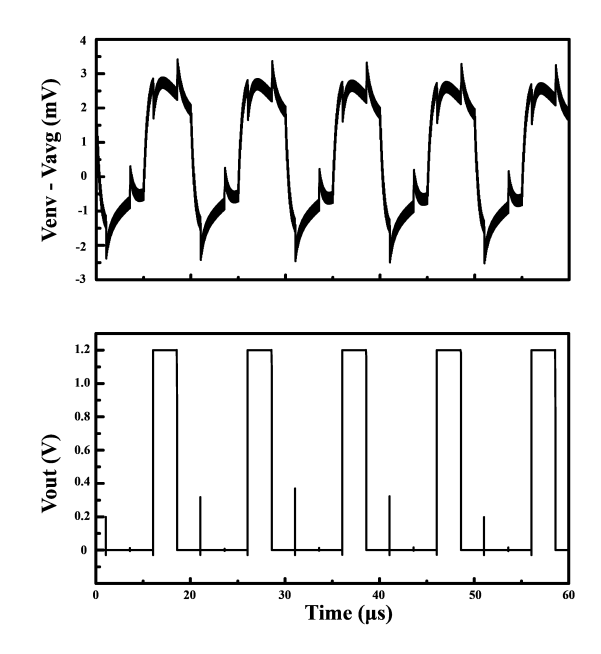


Fig. 4. Time waveform of the difference between the envelope and average signal at the output of the envelope detector and output of the comparator when amplitude of the input RF signal is 200 mV and MI is 1%.

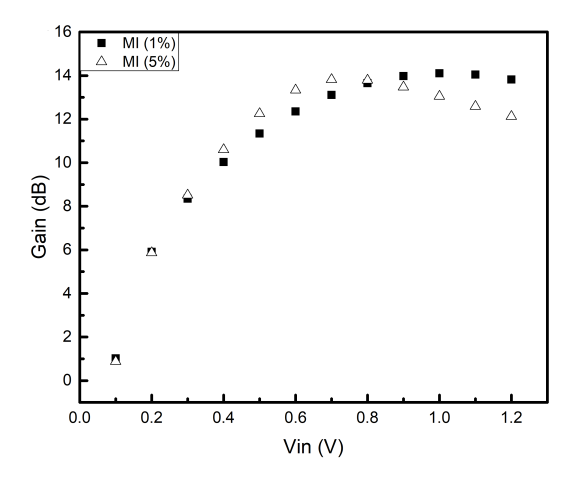


Fig. 5. Conversion gain as the function of the input voltage amplitude when modulation index is 1% and 5%.

Firstly, the proposed ASK demodulator is simulated with the input RF signal with amplitude of 200 mV and 1% modulation index. The time waveform of the envelope signals,  $V_{env}$ , along with the output signal of the comparator, is illustrated Figure 4. The conversion gain for a different low modulation index, 1% and 5%, as a function of the amplitude of the input signal is shown in Figure 5. The conversion gain is almost constant in the entire input amplitude range, due to the self-biasing structure. To demonstrate the feasibility of resolving the low modulation index, we show the difference between the amplitude of the baseband signal after the envelope detector and the ripple voltage in Figure 6, as this is the signal that should be resolved by the comparator.

The simulated current consumption of the proposed de-

TABLE II
SUMMARY AND COMPARISON WITH LITERATURE

Name	Year	Process (nm)	Carrier freq (MHz)	Data rate Mbps	Power (µW)	MI %
[21]	2008	180	2	1	336	5.5
[15]	2016	130	915	2	<4.13	5
[22]	2017	180	5	0.5	17	5
[23]	2019	180	13.56	1	30	2.33
This Work	2019	65	90	0.05	0.075(@0.2V)	1

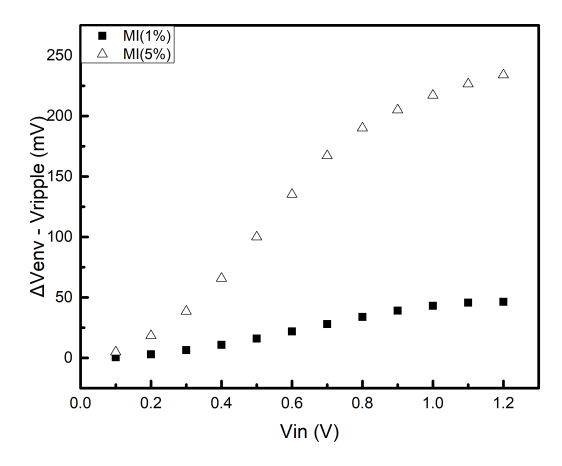


Fig. 6. The difference between the amplitude of the baseband signal after the envelope detector and the ripple voltage as a function of the input voltage amplitude.

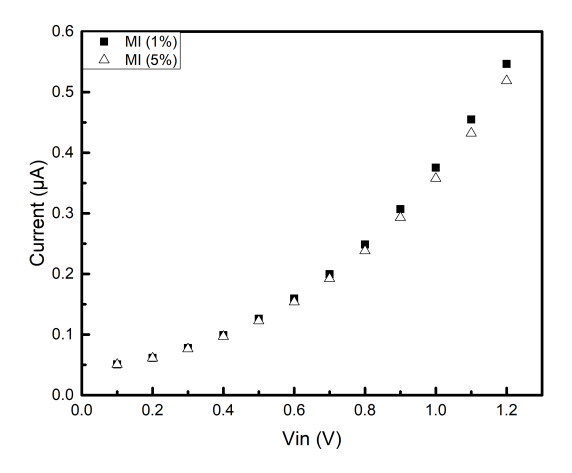


Fig. 7. The current consumption of the ASK demodulator as a function of the input voltage amplitude.

modulator is shown in Figure 7. The current increases with the input signal amplitude and the maximum value is around 550 nA at 1.2 V input amplitude. In the proposed implant-to-implant link, we are mostly concerned with a lower input amplitudes. For example, at the input amplitude of 200 mV, the current is lower than 70 nA, which represents significant power saving comparated with the adaptive bias based CS ASK demodulator [15].

In Table II, we compare the simulated results of the

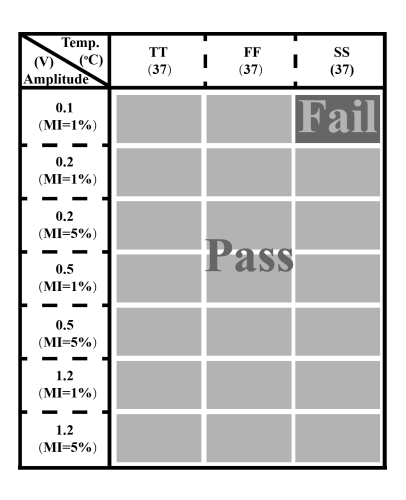


Fig. 8. Shmoo plot for the modulation indexes versus temperature variation under different process corners.

proposed ASK demodulator with the experimental results of the ASK demodulators that can resolve input signals with low modulation index. The proposed design resolves the low modulation index at the lowest cost of the power consumption.

Due to the low variation in the temperature of the human brain, a temperature  $37^{\circ}C$  is chosen for the operating temperature of the mm-sized IMDs. To evaluate robustness of the proposed ASK demodulator the Shmoo plot in Figure 8 depicts three corners of operation, typical-typical(TT), fast-fast(FF) and slow-slow(SS). The proposed circuit only fails at SS corner with 100 mV input amplitude and 1% modulation index, due to the reduced leakage current of transistor  $M_6$  at SS corner.

### IV. CONCLUSION

Self-biased common-source based envelope detector enables the implant device to resolve a low modulation index input RF signal at low power consumption. The proposed demodulator, along with a impedance switching modulator, will be integrated with on-chip coil in order to experimentally demonstrate the feasibility of the implant to implant link in the future work. Characterization of this link will enable further advances in the design of the distributed closed-loop system of mm-sized implants.

# ACKNOWLEDGMENT

This research was supported by the National Science Foundation under grant number CNS-1763843.

#### REFERENCES

- S. Ha, A. Akinin, J. Park, C. Kim, H. Wang, C. Maier, P. P. Mercier, and G. Cauwenberghs, "Silicon-integrated high-density electrocortical interfaces," *Proceedings of the IEEE*, vol. 105, no. 1, pp. 11–33, Jan 2017
- [2] M. Yin, D. A. Borton, J. Aceros, W. R. Patterson, and A. V. Nurmikko, "A 100-channel hermetically sealed implantable device for chronic wireless neurosensing applications," *IEEE transactions on biomedical* circuits and systems, vol. 7, no. 2, pp. 115–128, 2013.
- [3] D. Ahn and M. Ghovanloo, "Optimal design of wireless power transmission links for millimeter-sized biomedical implants," *IEEE transactions on biomedical circuits and systems*, vol. 10, no. 1, pp. 125–137, 2015.
- [4] A. Khalifa, Y. Karimi, Q. Wang, S. Garikapati, W. Montlouis, M. Stanaćević, N. Thakor, and R. Etienne-Cummings, "The microbead: A highly miniaturized wirelessly powered implantable neural stimulating system," *IEEE transactions on biomedical circuits and systems*, vol. 12, no. 3, pp. 521–531, 2018.
- [5] N. Ahmadi, M. L. Cavuto, P. Feng, L. B. Leene, M. Maslik, F. Mazza, O. Savolainen, K. M. Szostak, C.-S. Bouganis, J. Ekanayake et al., "Towards a distributed, chronically-implantable neural interface," in 2019 9th International IEEE/EMBS Conference on Neural Engineering (NER). IEEE, 2019, pp. 719–724.
- [6] V. W. Leung, L. Cui, S. Alluri, J. Lee, J. Huang, E. Mok, S. Shellhammer, R. Rao, P. Asbeck, P. P. Mercier, L. Larson, A. Nurmikko, and F. Laiwalla, "Distributed microscale brain implants with wireless power transfer and mbps bi-directional networked communications," in 2019 IEEE Custom Integrated Circuits Conference (CICC), April 2019, pp. 1–4
- [7] G. C. McConnell, H. D. Rees, A. I. Levey, C.-A. Gutekunst, R. E. Gross, and R. V. Bellamkonda, "Implanted neural electrodes cause chronic, local inflammation that is correlated with local neurodegeneration," *Journal of neural engineering*, vol. 6, no. 5, p. 056003, 2009.
- [8] A. Prasad, Q.-S. Xue, V. Sankar, T. Nishida, G. Shaw, W. J. Streit, and J. C. Sanchez, "Comprehensive characterization and failure modes of tungsten microwire arrays in chronic neural implants," *Journal of neural engineering*, vol. 9, no. 5, p. 056015, 2012.
- [9] M. Ghovanloo and K. Najafi, "A wideband frequency-shift keying wireless link for inductively powered biomedical implants," *IEEE Trans*actions on Circuits and Systems I: Regular Papers, vol. 51, no. 12, pp. 2374–2383, Dec 2004.
- [10] M. Kiani and M. Ghovanloo, "A 20-mb/s pulse harmonic modulation transceiver for wideband near-field data transmission," *IEEE Transactions on Circuits and Systems II: Express Briefs*, vol. 60, no. 7, pp. 382–386, July 2013.
- [11] Yamu Hu and M. Sawan, "A fully integrated low-power bpsk demodulator for implantable medical devices," *IEEE Transactions on Circuits* and Systems I: Regular Papers, vol. 52, no. 12, pp. 2552–2562, Dec 2005.
- [12] C. Wang, C. Chen, R. Kuo, and D. Shmilovitz, "Self-sampled all-mos ask demodulator for lower ism band applications," *IEEE Transactions* on Circuits and Systems II: Express Briefs, vol. 57, no. 4, pp. 265–269, April 2010.
- [13] Y. Karimi, A. Athalye, S. Das, P. M. Djurić, and M. Stanaćević, "Design of backscatter-based tag-to-tag system," in *IEEE International Conference on RFID (RFID)*, 2017.
- [14] X. Sha, Y. Karimi, P. M. Djurić, M. Stanacevic, and S. R. Das, "Study of Mm-Sized coil to coil backscatter based communication link," in 2019 IEEE 10th Annual Ubiquitous Computing, Electronics & Mobile Communication Conference (UEMCON) (IEEE UEMCON 2019), Columbia University, New York, USA, Oct. 2019.
- [15] V. Fiore, E. Ragonese, and G. Palmisano, "Low-power ask detector for low modulation indexes and rail-to-rail input range," *IEEE Transactions* on Circuits and Systems II: Express Briefs, vol. 63, no. 5, pp. 458–462, May 2016.
- [16] S. B. Sleiman and M. Ismail, "Transceiver parameter detection using a high conversion gain rf amplitude detector," in *Proceedings of 2010 IEEE International Symposium on Circuits and Systems*, May 2010, pp. 2059–2062.
- [17] M. van Elzakker, E. van Tuijl, P. Geraedts, D. Schinkel, E. Klumperink, and B. Nauta, "A 1.9w 4.4fj/conversion-step 10b 1ms/s charge-redistribution adc," in 2008 IEEE International Solid-State Circuits Conference Digest of Technical Papers, Feb 2008, pp. 244–610.

- [18] D. Jiang, D. Cirmirakis, M. Schormans, T. A. Perkins, N. Donaldson, and A. Demosthenous, "An integrated passive phase-shift keying modulator for biomedical implants with power telemetry over a single inductive link," *IEEE Transactions on Biomedical Circuits and Systems*, vol. 11, no. 1, pp. 64–77, Feb 2017.
- [19] P. P. Wang, H. Jiang, L. Gao, P. Sen, Y. Kim, G. M. Rebeiz, P. P. Mercier, and D. A. Hall, "A near-zero-power wake-up receiver achieving 69-dbm sensitivity," *IEEE Journal of Solid-State Circuits*, vol. 53, no. 6, pp. 1640–1652, June 2018.
- [20] A. Shrivastava and B. H. Calhoun, "A 150nw, 5ppm/o c, 100khz on-chip clock source for ultra low power socs," in *Proceedings of the IEEE 2012* Custom Integrated Circuits Conference, Sep. 2012, pp. 1–4.
- [21] C. A. Gong, M. Shiue, K. Yao, T. Chen, Y. Chang, and C. Su, "A truly low-cost high-efficiency ask demodulator based on self-sampling scheme for bioimplantable applications," *IEEE Transactions on Circuits* and Systems 1: Regular Papers, vol. 55, no. 6, pp. 1464–1477, July 2008.
- [22] M. L. Navaii, M. Jalali, and H. Sadjedi, "A 34-pj/bit area-efficient ask demodulator based on switching-mode signal shaping," *IEEE Transac*tions on Circuits and Systems II: Express Briefs, vol. 64, no. 6, pp. 640–644, June 2017.
- [23] D. Wang, J. Hu, and J. Wu, "An hf passive rfid tag ic with low modulation index ask demodulator," *IEEE Transactions on Industrial Electronics*, vol. 66, no. 3, pp. 2164–2173, March 2019.